Journal of Electron Spectroscopy and Related Phenomena xxx (2014) xxx–xxx

Contents lists available at ScienceDirect

Journal of Electron Spectroscopy and Related Phenomena

journal homepage: www.elsevier.com/locate/elspec

Unoccupied electronic structure and relaxation dynamics of Pb/Si(1 1 1)

M. Sandhofer[a], I.Yu. Sklyadneva[b,c], V. Sharma[a,1], V. Mikšić Trontl[a], P. Zhou[a], M. Ligges[a], R. Heid[d], K.-P. Bohnen[d], E.V. Chulkov[b,e], U. Bovensiepen[a,*]

[a] Faculty of Physics and Center for Nanointegration (CENIDE), University of Duisburg-Essen, 47048 Duisburg, Germany
[b] Donostia International Physics Center (DIPC), Paseo de Manuel Lardizabal 4, 20018 San Sebastian/Donostia, Basque Country, Spain
[c] Tomsk State University, 6340501 Tomsk, Russian Federation
[d] Karlsruher Institut für Technologie, Institut für Festkörperphysik, D-76021 Karlsruhe, Germany
[e] Centro de Física de Materiales CFM – Materials Physics Center MPC, Centro Mixto CSIC-UPV/EHU, 20018 San Sebastian/Donostia, Spain

ARTICLE INFO

Article history:
Available online xxx

Keywords:
Unoccupied band structure
Pb/Si(1 1 1)
Quantum well states
Nonlinear photoemission
Density functional theory
Femtosecond dynamics

ABSTRACT

The unoccupied electronic structure of epitaxial Pb films on Si(1 1 1) is analyzed by angle-resolved two-photon photoemission in the $\bar{\Gamma} \rightarrow \bar{M}$ direction close to the Brillouin zone center. The experimental results are compared to density functional theory calculations and we focus on the nature of the interaction of the $6p_z$ states with the Si substrate. The experimentally obtained dispersion $E(k_{||})$ of the unoccupied quantum well states is weaker than expected for freestanding films, in good agreement with their occupied counterparts. Following $E(k_{||})$ of quantum well states as a function of momentum at different energies, which are degenerate and non-degenerate with the Si conduction band, we observe no influence of the Si bulk band and conclude a vanishing direct interaction of the Pb $6p_z$ states with the Si band. However, the momentum range at which mixing of $6p_z$ and $6p_{x,y}$ derived subbands is found to occur in the presence of the Si substrate is closer to $\bar{\Gamma}$ than in the corresponding freestanding film, which indicates a substrate-mediated enhancement of the mixing of these states. Additional femtosecond time-resolved measurements show a constant relaxation time of hot electrons in unoccupied quantum well states as a function of parallel electron momentum which supports our conclusion of a $p_{x,y}$ mediated interaction of the p_z states with the Si conduction band.

© 2014 Published by Elsevier B.V.

1. Introduction

Laser-based photoemission spectroscopy complements well-established static photoemission techniques. Laser light sources offer a high photon flux, promise an increased bulk sensitivity due to the low photon energy [1] and are, therefore, suitable to investigate buried interfaces [2,3]. Excellent resolution and sensitivity was also demonstrated for complex materials [4,5]. The availability of femtosecond pulses from broad band laser light sources was naturally essential for the detailed insight obtained in ultrafast surface dynamics [6].

Two-photon photoemission spectroscopy (2PPE) of unoccupied electronic states is very successful regarding the investigation of surface and interface properties [7–9,6]. By now such non-linear photoemission is a well established tool which we employ here for an analysis of the unoccupied electronic structure of epitaxial Pb films grown on Si(1 1 1), in order to complement existing studies of the occupied electronic structure.

Pb grown on Si(1 1 1) is a widely investigated model system for a metallic film on a semiconductor substrate, which has been studied e.g. by scanning tunneling microscopy and spectroscopy [10–13], photoemission spectroscopy [14–17], low energy electron diffraction (LEED) [18] and density-functional theory (DFT) [19]. This particular material system became well known for its electron mediated growth [20] and the "devil's staircase" structure at the interface [21]. The electronic structure of these Pb films is formed by quantum wells, which confine the electronic wave functions and quantize their energy for the direction perpendicular to the surface. A particular topic is the influence of the substrate on the electronic structure of these quantum well states (QWS). Absence of dispersion parallel to the surface $E(k_{||})$ is observed for the highest occupied QWS near $\bar{\Gamma}$ [22,16,23,24]. If compared to freestanding Pb films and

* Corresponding author. Tel.: +49 2033794566
E-mail address: uwe.bovensiepen@uni-due.de (U. Bovensiepen).
[1] Current address: Indian Institute of Technology – Hyderabad, ODF Estate, Yeddumailaram, Andhra Pradesh 502205, India.

http://dx.doi.org/10.1016/j.elspec.2014.04.006
0368-2048/© 2014 Published by Elsevier B.V.

Please cite this article in press as: M. Sandhofer, et al., Unoccupied electronic structure and relaxation dynamics of Pb/Si(1 1 1), J. Electron Spectrosc. Relat. Phenom. (2014), http://dx.doi.org/10.1016/j.elspec.2014.04.006

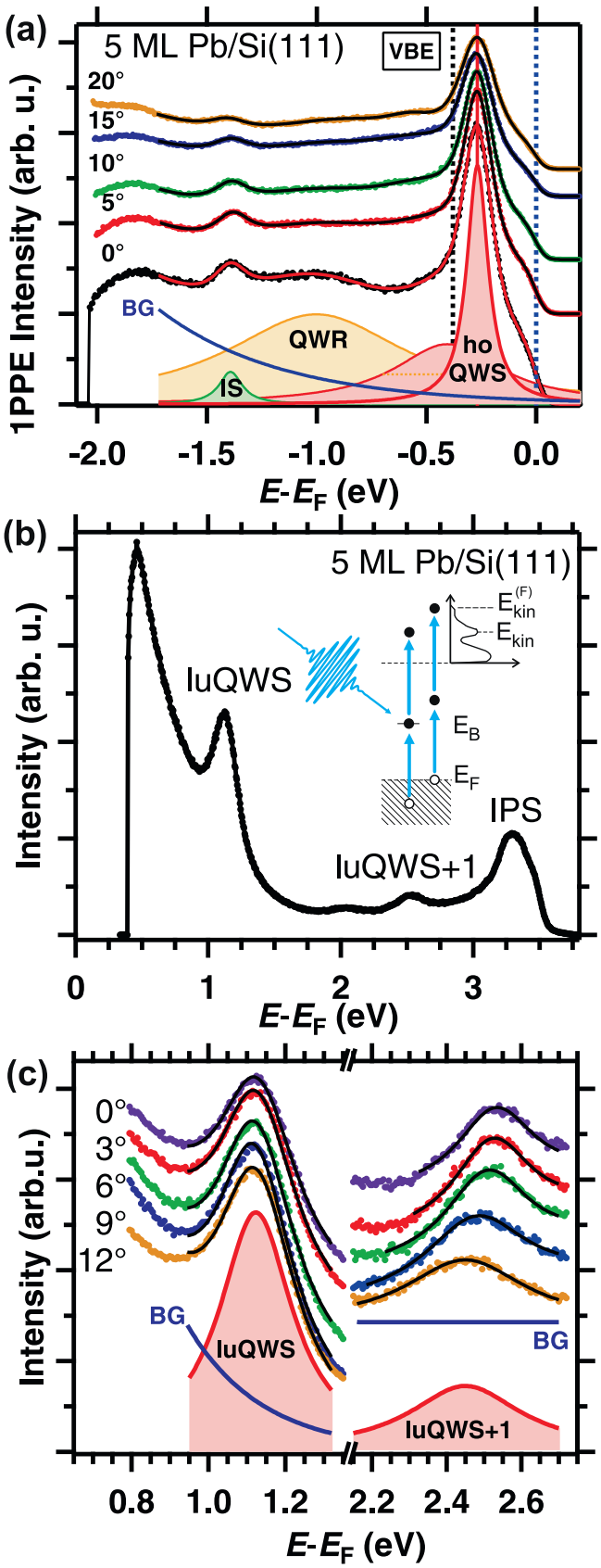

Fig. 1. Photoemission spectra for 5 ML coverage Pb/Si(1 1 1) taken with the time of flight spectrometer. (a) Direct photoemission intensity as a function of binding energy with respect to the Fermi level E_F for different photoemission angles. Points denote the data ($h\nu = 6.0$ eV), lines depict the fit to the data and shaded areas represent the composition of the fit for normal emission. In addition to the pronounced peak which is the highest occupied quantum well state (hoQWS), a broad quantum well resonance (QWR) and an interface state (IS) are observed. Because the hoQWS is partly degenerate with the Si valence band (valence band edge (VBE) indicated by vertical dashed black line), an additional Lorentzian is included. (b) One color 2PPE intensity as a function of $E - E_F$ at normal emission with the 2PPE scheme in the inset. The spectral features at $E - E_F = 1.15$ eV and 2.55 eV are the lowest unoccupied (lu) QWS and luQWS+1. The peak at 3.3 eV originates from the first image potential state (IPS). The small feature at 2.05 eV is a QWS contribution from 6 ML as explained in [28]. (c) One color 2PPE intensity as a function of $E - E_F$ for different photoemission angles for the luQWS and the luQWS+1. (For interpretation of the references to color in this figure legend, the reader is referred to the web version of this article.)

to Al, Mg and In films on Si(1 1 1) [25,26,16] this "flat dispersion" appears as unique for the Pb/Si(1 1 1) system.

Its origin is still under discussion. The QWSs of Pb/Si(1 1 1) investigated here are derived from 6*p* Pb bands in $\Gamma \rightarrow L$ direction. Hence, QWSs at the $\bar{\Gamma}$-point are of p_z symmetry (with z perpendicular to the surface). For increasing in-plane momentum towards $\bar{M}$ the QWS bands change character from p_z to $p_{x,y}$ symmetry [22,27–29]. While Upton et al. connect the flat dispersion to the anticrossing coupling with Si(1 1 1) valence bands [22], Dil et al. hold a high localization of the corresponding p_z orbitals responsible [27]. Recent work of Slomski et al. have investigated the influence of the interface by comparing the Pb/Si(1 1 1) band structure for different interface preparations, concluding a change of the in-plane lattice constant [30].

Here, we complement the existing work on the occupied electronic structure for Pb/Si(1 1 1) by analyzing the unoccupied part of the electronic structure. We perform time- and angle-resolved 2PPE on Pb/Si(1 1 1) and compare our results with density functional theory (DFT) calculations of Pb(1 1 1) films. We conclude a scenario, in which the electronic structure is determined by the Pb $6p_{x,y}$ derived states which interact directly with the Si(1 1 1) substrate. Due to the complex interface structure of Pb/Si(1 1 1) which deviates from the Pb(1 1 1) film case, these $p_{x,y}$ states mediate the interaction with states of p_z symmetry, which we probe in 2PPE near $\bar{\Gamma}$.

2. Sample preparation and experimental setup

The sample preparation and experimental setup has been described in detail earlier [17,31] and will be briefly summarized in this section. For the growth of epitaxial lead thin films on Si(1 1 1) we follow a well established routine. First the Si(1 1 1)-7×7 reconstruction is prepared under ultra high vacuum (base pressure $<1 \times 10^{-10}$ mbar) conditions. Evaporation of 1/3 monolayers (ML) Pb from a Knudsen cell saturates the Si(1 1 1) dangling bonds resulting in the $\beta - \sqrt{3} \times \sqrt{3}$ (henceforth $\sqrt{3}$) reconstruction [32]. Subsequently, Pb(1 1 1) films are grown, using the $\sqrt{3}$ reconstructed Si surface as a seed layer for epitaxial growth. The sample temperature T was held at $T = 100$ K during preparation to avoid formation of islands by limiting Pb atom diffusion [20,33]. The deposition rate was monitored by a quartz balance and the surface quality was checked using LEED. Pb wedges have been grown with a lateral thickness gradient of <0.5 ML/mm to obtain a quasi-continuous thickness variation in order to investigate discrete integer thicknesses of the film [34]. The actual coverage was determined by analysis of the binding energy and photoemission intensity of occupied QWS [31,22] using linear photoemission spectroscopy (see below).

For the investigation of the electronic structure of these thin films by laser-based photoelectron spectroscopy a commercial amplified Ti:Sa ultrashort pulse laser system operating at a repetition rate of 250 kHz (Coherent RegA 9040) and $\lambda = 818$ nm central wavelength was used. It provided 40 fs laser pulses at 6 μJ energy per pulse. For linear photoemission (1PPE) the fundamental

Please cite this article in press as: M. Sandhofer, et al., Unoccupied electronic structure and relaxation dynamics of Pb/Si(1 1 1), J. Electron Spectrosc. Relat. Phenom. (2014), http://dx.doi.org/10.1016/j.elspec.2014.04.006

RegA output was frequency doubled by two consecutive β barium borate (BBO) crystals, leading to a photon energy of $h\nu = 6.0$ eV. For monochromatic 2PPE an optical parametric amplifier (OPA) was used to convert the RegA output into $h\nu = 1.9$ eV which was frequency doubled to 3.8 eV. Typical fluences of the 6.0 eV and 3.8 eV beams are <2 μJ/cm^2. For bi-chromatic time-resolved (tr) 2PPE the fundamental output of the RegA was combined with the frequency doubled OPA output ($h\nu_2 = 3.9$ eV) providing pump and probe pulses. The beams were focused into the UHV chamber with typical focus diameters of 100 μm. Pump and probe laser pulses are overlapped in space and time and are delayed with respect to each other by an optical path length difference. Typical fluences of the RegA fundamental output on the sample were 70 μJ/cm^2.

The kinetic energy of photo-emitted electrons in static photoemission were measured by an electron time-of-flight spectrometer (TOF) with a channel plate anode and ±3° acceptance angle. The overall energy resolution is 70 meV with contributions from the TOF (10 meV at $E_{kin} = 1$ eV) and the bandwidth of ultrashort laser pulses (OPA 2nd harmonic: 40 meV, RegA fundamental: 60 meV). Angle dependent spectra were measured and respective spectral features were assigned to the respective electron momentum component $\hbar k_{||} = \sqrt{2m_e E_{kin}}\sin(\theta)$; $k_{||}$ denoting momenta parallel to the surface in direction $\bar{\Gamma} \rightarrow \bar{M}$, m_e the electron mass, E_{kin} the kinetic energy of the photoelectron and θ the tilting angle of the sample surface normal with respect to the spectrometer axis.

Furthermore, combined angle- and time-resolved data were obtained by a position sensitive time-of-flight spectrometer (pTOF) to exploit the instrument's promising conditions regarding 2PPE spectroscopy. The pTOF utilizes a commercial position sensitive delay line anode (RoentDec Hexanode) to detect the arrival time of individual electrons and their position on the detector from which the angle θ is derived. Hence, we acquire 4-dimensional data sets of the photoemission intensity $I(E, t, k_x, k_y)$ as a function of energy, time and two mutually perpendicular in-plane momentum components in x and y direction with a momentum resolution up to 0.002 Å^{-1} and an energy resolution comparable to the above given value. For details on the pTOF see [35]. Note that both spectrometers are mounted in the same vacuum chamber and can be used alternatively.

3. Results and discussion

For sample characterization and as a reference, 1PPE is employed to probe the occupied electronic structure. Typical spectra are shown for selected photoemission angles in Fig. 1(a). These spectra were taken on 5 ML Pb/Si(1 1 1) for $\theta = 0°$ to 20° emission angle using a photon energy of $h\nu = 6.0$ eV. The high-energy cutoff is identified as the Fermi level E_F and is taken as an energy reference to set the energy scale from the measured E_{kin} to a negative binding energy $E - E_F$. The slowest electrons at the low-energy cutoff (secondary edge) at $E - E_F = -2.04$ eV overcome the binding energy of $E_B = 2.04$ eV and the work function Φ before being detected. Considering energy conservation $h\nu = 6.0$ eV $= \Phi + 2.04$ eV results in a work function of $\Phi = 3.96$ eV.

Three spectral features are prominent: an interface state at $E - E_F = -1.39$ eV, a quantum well resonance (QWR) at $E - E_F = -1$ eV, and the highest occupied (ho) QWS at $E - E_F = -0.27$ eV. To determine the binding energies all spectra where fitted by an exponential background (solid blue line BG) and Lorentz profiles (filled curves) for the peaks multiplied by the Fermi Dirac distribution and convoluted by a Gaussian instrument resolution function. The interface state is visible at the same binding energy throughout all coverages in agreement with [3]. The hoQWS is changing its binding energy in a range of 6 meV for photoemission angles between $\theta = 0°$ and 20°, i.e. this state exhibits a weak dispersion with $\hbar k_{||}$ in agreement with previous studies in the measured momentum region [22].

We now turn to our 2PPE results. First we will discuss angle dependent 2PPE and our results on the unoccupied electronic structure of Pb/Si(1 1 1). The experimentally determined $E(k_{||}) > E_F$ will be compared with results of the DFT calculations. Subsequently, we present time-resolved results as a function of $k_{||}$ and discuss the observed momentum-dependence of the population dynamics.

Fig. 1(b) shows a schematic of the 2PPE process in the inset and an exemplary 2PPE spectrum ($h\nu = 3.8$ eV). The inset illustrates the binding energy determination for the unoccupied QWS. The fastest electrons in the 2PPE spectrum are photo-emitted by absorption of two photons from the Fermi level to a final state with kinetic energy E^F_{kin} following $2h\nu = E^F_{kin} + \Phi$. An electron at a normally unoccupied state absorbs a photon of energy $h\nu$, overcomes the remaining potential barrier $\Phi - E_B$ and is detected at the kinetic energy of $E^B_{kin} = h\nu - (\Phi - E_B)$. As a consequence, the binding energy with respect to E_F of intermediate states at E^B_{kin} are calculated by $E_B = -E^F_{kin} + h\nu + E^B_{kin}$.

In the 2PPE spectrum in Fig. 1(b) the peaks at $E - E_F = 1.15$ eV and 2.55 eV are identified as lowest unoccupied (lu) QWS and luQWS+1, respectively, following [28]. The peak at $E - E_F = 3.3$ eV originates from the first image potential state (IPS) in agreement with [31]. Here, we extend our previous work by angle-resolved 2PPE and analyze unoccupied QWSs and their momentum dispersion $E(k_{||})$. Fig. 1(c) shows 2PPE spectra for different photoemission angles $\theta = 0°, \ldots, 20°$ for the two unoccupied QWSs of Fig. 1(b). The peak energy is determined by a fit function (black line on data points) composed of an Gaussian instrument resolution function convoluted with an exponential background function (solid line BG) to which a Lorentz curve is added to account for the photoemission line (filled line).

Fig. 2 shows the obtained dispersion $E(k_{||})$ for the three investigated QWSs. The error in binding energy of the unoccupied

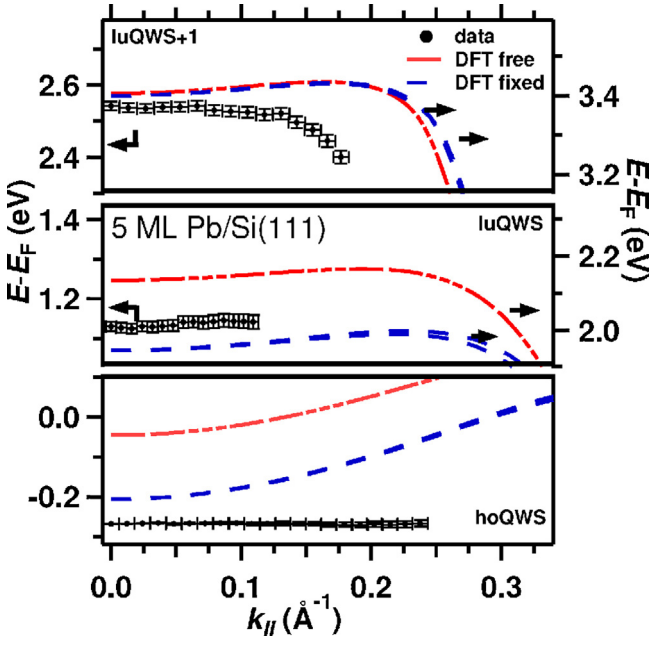

Fig. 2. Unoccupied electronic structure of 5 ML Pb/Si(1 1 1). The binding energy of quantum well states (QWSs) of 5 ML Pb/Si(1 1 1) coverage versus $k_{||}$ ($\bar{\Gamma} \rightarrow \bar{M}$). Points denote the fitting results of Fig. 1 with error bars, dashed lines are density functional theory (DFT) calculations as indicated by the legend (see text for details). For better visibility the energy axis is separated into three regions, zooming into QWS binding energies. Because the binding energies of the calculations and experiment differ by ≈1 eV, unoccupied states of DFT calculations are shown using an additional energy axis on the right side with energy offset compared to the left axis.

Please cite this article in press as: M. Sandhofer, et al., Unoccupied electronic structure and relaxation dynamics of Pb/Si(1 1 1), J. Electron Spectrosc. Relat. Phenom. (2014), http://dx.doi.org/10.1016/j.elspec.2014.04.006

Table 1
Changes in the interlayer distances in % of the bulk value: $\Delta d_{ij} = (d_{ij} - d_{bulk})/d_{bulk}$.

	Δd_{12}	Δd_{23}	Δd_{34}	Δd_{45}
Free DFT	−5.6	+0.2	+0.2	−5.6
Fixed DFT	−4.1	+1.0	≃0	0.0

states is calculated from uncertainties of the fit and systematic errors due to the sample to TOF geometry. The experimental binding energies of the hoQWS, luQWS and luQWS+1 at the $\bar{\Gamma}$ point are $E - E_F = -0.27$ eV, 1.13 eV and 2.54 eV, respectively. The luQWS exhibits a weak dispersion of 12 meV in momentum range from 0 up to 0.11 Å^{-1} which is in the limit of our error bars (see Fig. 2). The luQWS+1 exhibits clearly a negative momentum dispersion. Up to $k_{||} = 0.13$ Å^{-1} its binding energy decreases by 20 meV and from there it suddenly drops by 120 meV until $k_{||} = 0.17$ Å^{-1}.

To estimate the influence of the substrate on the Pb electron band dispersion we performed DFT calculations for two theoretical model systems: a freestanding lead film (free DFT calculation) with atomic positions relaxed in the direction perpendicular to the surface and a freestanding Pb film with interlayer spacing fixed on one side to the Pb bulk value to simulate the influence of the substrate (fixed DFT calculation).

The Pb(1 1 1) films are modeled by a supercell geometry. The repeated films are composed of 5–10 Pb(1 1 1) layers and are separated by a vacuum corresponding to 7.5 atomic layers. The atomic positions within the layers maintain the symmetry of the bulk, and their lateral positions are fixed at the theoretical bulk lattice parameter obtained by total-energy minimization [36]. Along the stacking direction, the positions of Pb(1 1 1) layers are relaxed until the forces between atomic layers become smaller than 10^{-4} Ry a.u.$^{-1}$. In the free DFT calculation, both sides of a film are allowed to relax. In the fixed DFT calculation, only one side of a film is relaxed while at the other side the first interlayer distance is kept fixed at the lead bulk value. The relaxation consists of a contraction of the first (topmost) spacing (d_{12}) relative to the bulk distance and an expansion of the second one (d_{23}), regardless of the film thickness [37]. To show the difference between the free and fixed DFT calculations the structural surface relaxation for 5 ML Pb(1 1 1) films are given in Table 1. We note that experimental data on the interlayer spacing obtained by dynamical LEED [38] are in good agreement with the results of the DFT calculation for the fixed configuration.

The resulting binding energies of the free DFT calculation of the hoQWS, luQWS and luQWS+1 at the $\bar{\Gamma}$ point are $E - E_F = -0.05$ eV, 2.14 eV, and 3.41 eV, respectively (see Fig. 2). The binding energies of the fixed DFT calculation of the hoQWS, luQWS and luQWS+1 at the $\bar{\Gamma}$ point are $E - E_F = -0.21$ eV, 1.95 eV, and 3.40 eV, respectively.

Comparing these calculations, the fixation of the first Pb layer simulating an influence of the substrate along the normal coordinate reduces the binding energy of the hoQWS and the luQWS by 0.26 eV and 0.19 eV, respectively. The binding energy of the luQWS+1 is lowered by only 6 meV. The change in $E(k_{||})$ between

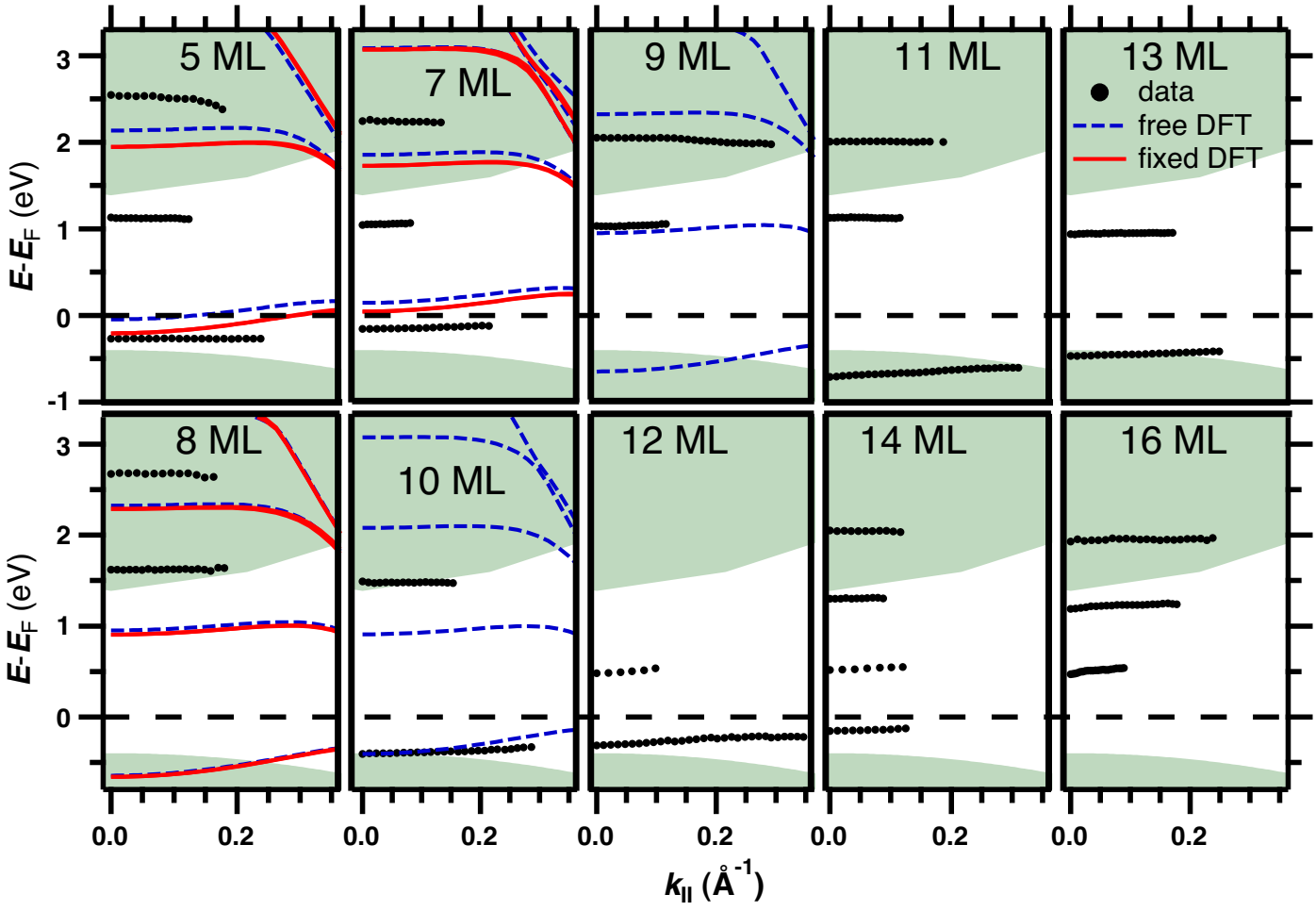

Fig. 3. Electronic structure below and above E_F for 5–16 ML Pb/Si(1 1 1) along $\bar{\Gamma} \rightarrow \bar{M}$. The upper panels show odd numbers of ML coverage, whereas the lower row of panels show even numbers of ML coverage. Black points denote experimental data, the different lines indicate free and fixed DFT calculations. The shaded areas highlight the Si projected bulk bands taken from literature [39]. The long dashed line at $E - E_F = 0$ eV marks the Fermi energy.

Please cite this article in press as: M. Sandhofer, et al., Unoccupied electronic structure and relaxation dynamics of Pb/Si(1 1 1), J. Electron Spectrosc. Relat. Phenom. (2014), http://dx.doi.org/10.1016/j.elspec.2014.04.006

the free and fixed case is negligible in the vicinity of the $\bar{\Gamma}$-point. The general structure of all DFT calculated bands is an electron-like behavior around the $\bar{\Gamma}$-point and a sudden turn to a downward dispersion at higher parallel electron momentum.

We now compare the experimental findings with these calculations. At first we recognize that the experimentally determined binding energies of luQWS and luQWS+1 are about 1 eV lower than calculated which we attribute to interaction between film and substrate. The lower theoretical binding energy obtained for the fixed case compared to the free case reproduces this trend towards lower binding energy for interaction with the substrate correctly. To obtain the correct values this interaction is likely required to be considered quantitatively, which is beyond the present study. Nevertheless the momentum dependence provides further information on this substrate-film interaction. The experimentally determined luQWS+1 binding energy (Fig. 2) exhibits a downward dispersion from $k_{||} = 0.13$ Å $^{-1}$ onwards. The fixed DFT calculations show a stronger downward dispersion starting at larger $k_{||} > 0.22$ Å $^{-1}$. This difference suggests that mixing of p_z and $p_{x,y}$ derived states is stronger and extends further towards $\bar{\Gamma}$ than for freestanding films. As investigated earlier in [30] the explanation could be a simple change in the in-plane lattice distance of the Pb film induced by the substrate. However, the Pb–Si(1 1 1) interface is complex and is to be considered as three dimensional. Therefore, a Si induced in plane lattice constant variation of the Pb film might represent an effective way to parameterize rather involved substrate induced effects like reconstruction and relaxation at a buried interface.

To understand the strong mixing between p_z and $p_{x,y}$ derived states, we proceed by discussing the unoccupied band structure for different Pb film thicknesses (5–16 ML) in comparison to the Si bulk bands in Fig. 3. The upper panels show experimental data (black points), DFT calculations for the free (dashed blue lines) and fixed (solid red lines) cases with coverage of odd number of ML. The lower row depicts results for even number of ML. The obtained binding energies are in agreement with Kirchmann and Bovensiepen [31]. We observe that the general behavior of the dispersion with momentum is for all thicknesses similar to that of the 5 ML case discussed above. All unoccupied QWS bands show a weak dispersion $E(k_{||})$ in the vicinity of the $\bar{\Gamma}$-point. In particular, for unoccupied QWS the dispersion is not modified by the Si bulk bands in the vicinity of the Si conduction band edge. The situation for 8 and 10 ML, where the luQWS is directly at the energy of the conduction band edge, provides a good argument for absence of direct coupling between Si states and the p_z derived Pb states [22]. Hence, the change in the degree of interaction with the $p_{x,y}$ states cannot be explained by the Si electronic structure alone.

We rather include the atomic structure of the $\beta - \sqrt{3}$ reconstruction into our considerations. As shown by Chan et al. [32] in the T4 model, the saturation of all Si(1 1 1) dangling bonds is achieved by the 1/3 ML Pb through bonds with the first Si layer which deviate from the direction perpendicular to the surface. Therefore the p_z fraction of the Si orbitals is reduced at the interface in favor of the $p_{x,y}$ fraction, resulting in a smaller orbital overlap with Pb $6p_z$ orbitals and a direct coupling of Pb $6p_{x,y}$ states with the Si ones. The Si atom in the second Si layer positioned directly underneath a particular Pb atom at the interface is forming an sp^3 hybrid orbital structure. Since the orbitals of this hybrid bind with Si atoms in the first Si layer, they are pointing into directions different from the surface normal. Consequently, there is little direct overlap of the Si orbitals of the second Si layer with the Pb p_z orbital, as well. Together with our findings of absent $6p_z$ electron interaction with the Si conduction band and that the mixing with the $6p_{x,y}$ states arises earlier in momentum space (Fig. 2, top panel) we conclude that the $6p_{x,y}$ electrons at the Pb/Si interface interact with Si directly

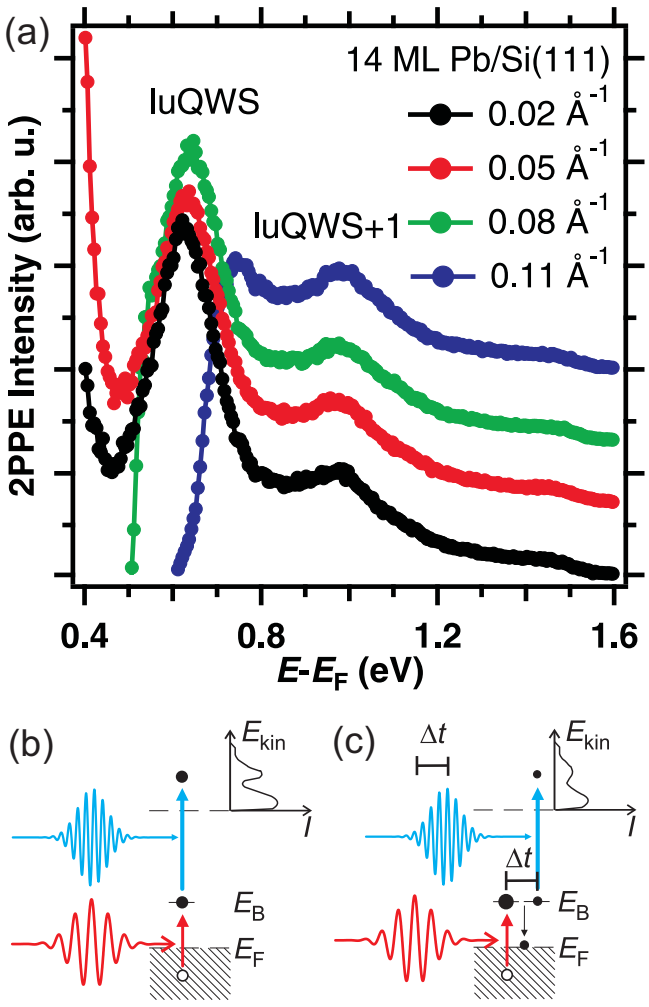

Fig. 4. Photoemission spectra for 14 ML Pb/Si(1 1 1) taken with the position sensitive time of flight spectrometer. (a) Two color 2PPE intensity as a function of $E - E_F$ for different $k_{||}$ integrated over the pump probe delay between −90 fs and 100 fs. An exponential background is subtracted. The spectral features at $E - E_F = 0.64$ eV and 0.98 eV denote lowest unoccupied quantum well state (luQWS) and luQWS+1, respectively. (b, c) Experimental schemes for time-resolved 2PPE without and with time delay between pump and probe pulses. (For interpretation of the references to color in this figure legend, the reader is referred to the web version of this article.)

and that this interaction alters the electronic structure of the p_z states.

After the discussion of the unoccupied QWS electronic structure we proceed to the relaxation dynamics investigated in a time-resolved 2PPE experiment. Here we investigate the momentum dependent relaxation dynamics of hot electrons in unoccupied QWSs of Pb/Si(1 1 1) by employing the pTOF spectrometer described above [35]. The advantage of this instrument is, that a broad range of electron momenta can be analyzed simultaneously without changing the sample-spectrometer geometry. For a comparison with the TOF data in Fig. 1(c), we show 2PPE spectra for 14 ML Pb/Si(1 1 1) at different electron momenta obtained by the pTOF in Fig. 4 (a). The peak at $E - E_F = 0.64$ eV depicts the luQWS, the one at 0.98 eV can be assigned to the luQWS+1 of neighboring coverage as explained in [28]. Note, that the kinetic energy of the luQWS spectral feature is too small to be observed for $k_{||} > 0.11$ Å $^{-1}$.

Fig. 4(b) shows the two-color 2PPE scheme. Electrons are excited by the first laser pulse with energy $h\nu_{Pump} = 1.5$ eV from below the Fermi level and populate a state at energy E_B. A second laser pulse with the energy of $h\nu_{Probe} = 3.9$ eV excites the electron

Please cite this article in press as: M. Sandhofer, et al., Unoccupied electronic structure and relaxation dynamics of Pb/Si(1 1 1), J. Electron Spectrosc. Relat. Phenom. (2014), http://dx.doi.org/10.1016/j.elspec.2014.04.006

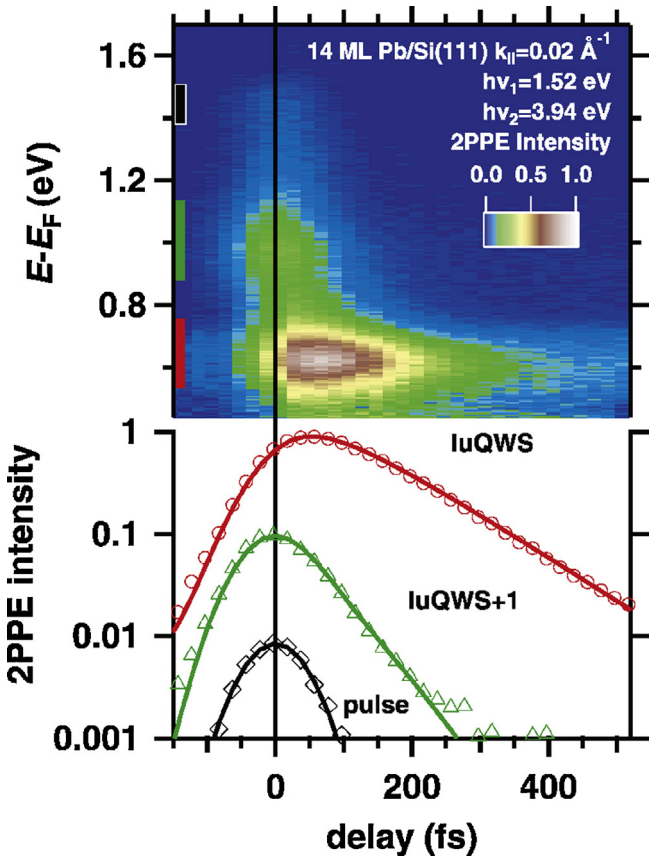

Fig. 5. Time and energy dependent 2PPE intensity and cross correlation traces for 14 ML Pb/Si(1 1 1) at $k_{||} = 0.02$ Å $^{-1}$. In the top panel a false color representation of 2PPE intensity as a function of intermediate state energy $E - E_F$ and pump-probe delay is shown. The data is shown with exponential background subtracted and normalized to the lowest unoccupied quantum well state (luQWS) peak intensity at $E - E_F = 0.64$ eV. The colored bars denote energy intervals over which the data was integrated to obtain the 2PPE intensity as a function of pump-probe delay, shown in the bottom panel. Three spectral regions are evaluated: the luQWS, the luQWS+1 and high energy electrons. The time dependence of the latter exhibits a good approximation to the laser pulse cross correlation. Solid lines are the fit by a rate equation model. (For interpretation of the references to color in this figure legend, the reader is referred to the web version of this article.)

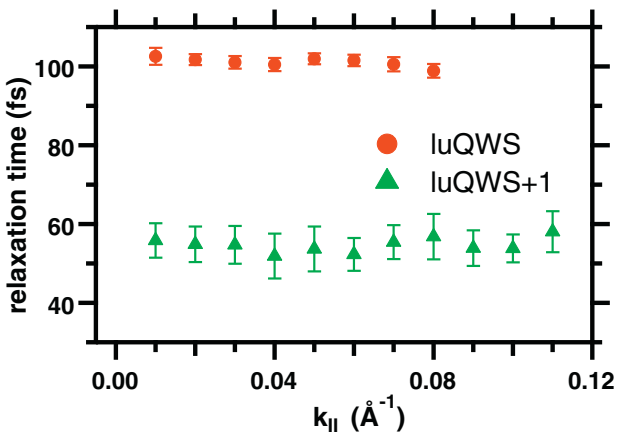

Fig. 6. Relaxation time of quantum well states (QWSs) of 14 ML coverage Pb/Si(1 1 1). The relaxation times are shown as a function of $k_{||}$ for the luQWS and luQWS+1 as indicated.

further to leave the sample. By changing the arrival time of the pump pulse with respect to the probe pulse, the population dynamics of intermediate states is analyzed directly in the time domain (Fig. 4(c)) [8]. In this way spectra for each delay Δt and parallel momentum component were taken. Such data are shown exemplarily for $k_{||} = 0.02$ Å $^{-1}$ in Fig. 5. The colored bars indicate the energy windows in which each spectral feature was analyzed, resulting in the time-dependent intensity trace in the panel below.

Following previous work [31] we describe the time-dependent intensity by a coupled rate equation model

$$\dot{n}_1(t) = -\Gamma_1 n_1(t) + \Gamma_{12} n_2(t) \quad (1)$$

$$\dot{n}_2(t) = -(\Gamma_{12} + \Gamma_2) n_2(t) \quad (2)$$

which takes intersubband scattering between the luQWS and the luQWS+1 into account.

$n_1(t)$ and $n_2(t)$ denote the population dynamics of the luQWS and luQWS+1, respectively. Γ_1 and Γ_2 describe the relaxation rate of the luQWS and luQWS+1, respectively, whereas Γ_{12} stands for the intersubband scattering rate coupling the luQWS+1 to the luQWS. The analytical solution follows from the above

$$n_2(t) = n_2^{(0)} e^{-(\Gamma_{12}+\Gamma_2)t} \quad (3)$$

$$n_1(t) = \underbrace{n_1^{(0)} e^{-\Gamma_1 t}}_{\text{population decay}} + \underbrace{n_2^{(0)} \frac{\Gamma_{12}}{\Gamma_2 + \Gamma_{12} - \Gamma_1} (e^{-\Gamma_1 t} - e^{-(\Gamma_{12}+\Gamma_2)t})}_{\text{population increase}} \quad (4)$$

In order to fit the data we assume $\Gamma_2 \ll \Gamma_{12}$. This leads to a direct coupling between the luQWS+1 and luQWS, where the remaining decay rate Γ_{12} of the luQWS+1 determines the characteristic delayed population rise of the luQWS (see Fig. 5). The resulting population dynamics is convoluted with a Gaussian laser pulse envelope and fitted to the data, which reproduces the data well as shown by the lines in the bottom panel of Fig. 5.

Fig. 6 depicts the obtained decay times of the luQWS and luQWS+1 as a function of $k_{||}$ and we conclude that these times are constant within error bars over the accessible momentum region. The average values of $\tau_1 = \hbar/\Gamma_1 = 102$ fs and $\tau_{12} = \hbar/\Gamma_{12} = 54$ fs are in agreement with earlier measurements at the $\bar{\Gamma}$ point with the TOF [28].

The observed constant relaxation times as a function of electron momentum support the absence of the coupling between Pb p_z subbands and Si bulk bands. As shown in Fig. 3 we observe for 14 ML film thickness a constant E_B as a function of $k_{||}$. Since the Si conduction band edge is shifting from the nearly degenerate case towards larger energy, the damping of the Pb QWS wave function in the Si bulk is expected to increase with $k_{||}$. This implies in case of a coupling of p_z derived QWS with the Si bulk states a relaxation channel which is expected to exhibit a momentum-dependent relaxation rate. The experimental time-resolved data show no indication of such a momentum-dependent relaxation. We rather explain the observed constant relaxation times by the constant relaxation phase space for e–e scattering due to the absence of a dispersion of the QWS state energy with $k_{||}$.

4. Summary

The unoccupied electronic structure of Pb/Si(1 1 1) has been investigated by angle dependent femtosecond time-resolved 2-photon-photoemission spectroscopy and density functional theory calculations. Substrate induced modifications in the binding energies of quantum well states are almost 1 eV. Albeit the changes in their dispersion $E(k_{||})$ are less pronounced, both effects highlight

Please cite this article in press as: M. Sandhofer, et al., Unoccupied electronic structure and relaxation dynamics of Pb/Si(1 1 1), J. Electron Spectrosc. Relat. Phenom. (2014), http://dx.doi.org/10.1016/j.elspec.2014.04.006

the importance of the substrate in understanding the electronic structure of this film-substrate system. We concluded that the interaction of the electronic quantum well states derived from Pb $6p_z$ orbitals with the Si substrate is mediated through the Pb $6p_{x,y}$ states, which couple directly with Si states. From our time-resolved analysis we conclude an absence of momentum dependent relaxation rates in the unoccupied quantum well states. While a substrate induced change in the interlayer spacing is in agreement with our observation, the complex interface structure might require consideration of reconstruction and relaxation effects.

Acknowledgements

This study was financially supported by the Deutsche Forschungsgemeinschaft through Sfb 616 and BO1823/2-2 and was partially supported by the Tomsk State University within the Competitiveness Improvement Program. We acknowledge fruitful discussions with P. Kratzer and experimental support by L. Rettig, I. Avigo, and S. Freutel.

References

[1] M.P. Seah, W.A. Dench, Surf. Interface Anal. 1 (1979) 2–11.
[2] C.H. Schwalb, S. Sachs, M. Marks, A. Schöll, F. Reinert, E. Umbach, U. Höfer, Phys. Rev. Lett. 101 (2008) 146801.
[3] L. Rettig, P.S. Kirchmann, U. Bovensiepen, New J. Phys. 14 (2012) 023047.
[4] T. Kiss, F. Kanetaka, T. Yokoya, T. Shimojima, K. Kanai, S. Shin, Y. Onuki, T. Togashi, C. Zhang, C.T. Chen, S. Watanabe, Phys. Rev. Lett. 94 (2005) 057001.
[5] J.D. Koralek, J.F. Douglas, N.C. Plumb, Z. Sun, A.V. Fedorov, M.M. Murnane, H.C. Kapteyn, S.T. Cundiff, Y. Aiura, K. Oka, H. Eisaki, D.S. Dessau, Phys. Rev. Lett. 96 (2006) 017005.
[6] U. Bovensiepen, H. Petek, M. Wolf (Eds.), Dynamics at Solid State Surfaces and Interfaces, Vol. 1. Current Developments, Wiley-VCH, Weinheim, Germany, 2010.
[7] T. Fauster, W. Steinmann, in: P. Halevi (Ed.), Photonic Probes of Surfaces, Electromagnetic Waves: Recent Developments in Research, Elsevier, Amsterdam, 1995, pp. 347–411.
[8] H. Petek, S. Ogawa, Prog. Surf. Sci. 56 (1997) 239–310.
[9] M. Weinelt, J. Phys.: Condens. Matter 14 (2002) R1099.
[10] C. Brun, I.-P. Hong, F. Patthey, I.Y. Sklyadneva, R. Heid, P.M. Echenique, K.P. Bohnen, E.V. Chulkov, W.-D. Schneider, Phys. Rev. Lett. 102 (2009) 207002.
[11] T. Zhang, P. Cheng, W.-J. Li, Y.-J. Sun, G. Wang, X.-G. Zhu, K. He, L. Wang, X. Ma, X. Chen, Y. Wang, Y. Liu, H.-Q. Lin, J.-F. Jia, Q.-K. Xue, Nat. Phys. 6 (2010) 104–108.
[12] J. Kim, C. Zhang, J. Kim, H. Gao, M.-Y. Chou, C.-K. Shih, Phys. Rev. B 87 (2013) 245432.
[13] I.-P. Hong, C. Brun, F. Patthey, I.Y. Sklyadneva, X. Zubizarreta, R. Heid, V.M. Silkin, P.M. Echenique, K.P. Bohnen, E.V. Chulkov, W.-D. Schneider, Phys. Rev. B 80 (2009) 081409(R).
[14] M. Jalochowski, H. Knoppe, G. Lilienkamp, E. Bauer, Phys. Rev. B 46 (1992) 4693.
[15] M.H. Upton, C.M. Wei, M.Y. Chou, T. Miller, T.-C. Chiang, Phys. Rev. Lett. 93 (2004) 026802.
[16] J.H. Dil, J.W. Kim, T. Kampen, K. Horn, A.R.H.F. Ettema, Phys. Rev. B 73 (2006) 161308.
[17] P.S. Kirchmann, M. Wolf, J.H. Dil, K. Horn, U. Bovensiepen, Phys. Rev. B 76 (2007) 075406.
[18] M. Yakes, M.C. Tringides, J. Phys. Chem. A 115 (2011) 7096–7104.
[19] C.M. Wei, M.Y. Chou, Phys. Rev. B 66 (2002) 233408.
[20] M. Hupalo, S. Kremmer, V. Yeh, L. Berbil-Bautista, E. Abram, M. Tringides, Surf. Sci. 493 (2001) 526–538.
[21] M. Yakes, V. Yeh, M. Hupalo, M.C. Tringides, Phys. Rev. B 69 (2004) 224103.
[22] M.H. Upton, T. Miller, T.-C. Chiang, Phys. Rev. B 71 (2005) 033403.
[23] S. Mathias, A. Ruffing, F. Deicke, M. Wiesenmayer, M. Aeschlimann, M. Bauer, Phys. Rev. B 81 (2010) 155429.
[24] A. Mans, J.H. Dil, A.R.H.F. Ettema, H.H. Weitering, Phys. Rev. B 66 (2002) 195410.
[25] L. Aballe, C. Rogero, P. Kratzer, S. Gokhale, K. Horn, Phys. Rev. Lett. 87 (2001) 156801.
[26] L. Aballe, C. Rogero, K. Horn, Surf. Sci. 518 (2002) 141–154.
[27] J.H. Dil, T.U. Kampen, B. Hülsen, T. Seyller, K. Horn, Phys. Rev. B 75 (2007) 161401.
[28] P.S. Kirchmann, L. Rettig, X. Zubizarreta, V.M. Silkin, E.V. Chulkov, U. Bovensiepen, Nat. Phys. 6 (2010) 782–785.
[29] M. Ligges, M. Sandhofer, I. Sklyadneva, R. Heid, K.P. Bohnen, S. Freutel, L. Rettig, P. Zhou, P.M. Echenique, E.V. Chulkov, U. Bovensiepen (submitted 2014).
[30] B. Slomski, F. Meier, J. Osterwalder, J.H. Dil, Phys. Rev. B 83 (2011) 035409.
[31] P.S. Kirchmann, U. Bovensiepen, Phys. Rev. B 78 (2008) 035437.
[32] T.-L. Chan, C.Z. Wang, M. Hupalo, M.C. Tringides, Z.-Y. Lu, K.M. Ho, Phys. Rev. B 68 (2003) 045410.
[33] H. Hong, L. Basile, P. Czoschke, A. Gray, T.-C. Chiang, Appl. Phys. Lett. 90 (2007) 051911.
[34] R.K. Kawakami, E. Rotenberg, H.J. Choi, E.J. Escorcia-Aparicio, M.O. Bowen, J.H. Wolfe, E. Arenholz, Z.D. Zhang, N.V. Smith, Z.Q. Qiu, Nature 398 (1999) 132–134.
[35] P.S. Kirchmann, L. Rettig, D. Nandi, U. Lipowski, M. Wolf, U. Bovensiepen, Appl. Phys. A 91 (2008) 211–217.
[36] R. Heid, K.-P. Bohnen, I.Y. Sklyadneva, E.V. Chulkov, Phys. Rev. B 81 (2010) 174527.
[37] I.Y. Sklyadneva, R. Heid, K.-P. Bohnen, P.M. Echenique, E.V. Chulkov, Phys. Rev. B 87 (2013) 085440.
[38] A. Mans, J.H. Dil, A.R.H.F. Ettema, H.H. Weitering, Phys. Rev. B 72 (2005) 155442.
[39] H. Weitering, T. Hibma, D. Heslinga, T. Klapwijk, Surf. Sci. 251–252 (1991) 616–620.

Please cite this article in press as: M. Sandhofer, et al., Unoccupied electronic structure and relaxation dynamics of Pb/Si(1 1 1), J. Electron Spectrosc. Relat. Phenom. (2014), http://dx.doi.org/10.1016/j.elspec.2014.04.006